

A. LISIŃSKA-CZEKAJ*, D. CZEKAJ*

SYNTHESIS OF $\text{Bi}_5\text{TiNbWO}_{15}$ CERAMICS

SYNTEZA CERAMIKI $\text{Bi}_5\text{TiNbWO}_{15}$

In the present study bismuth containing ceramic material $\text{Bi}_5\text{TiNbWO}_{15}$, belonging to the family of mixed-layer Aurivillius phases have been synthesized and fabricated. The compounds were synthesized according to the solid state reaction by mixed oxide method. The process of preparation was investigated by simultaneous thermal analysis and X-ray powder diffraction method. It was found that the structure adopted the polar orthorhombic space group $I2cm$, $a=5.4318\text{Å}$, $b=5.4255\text{Å}$, $c=41.6382\text{Å}$. Impedance spectroscopy was applied to characterize polarization processes present in the system and to separate the bulk, grain boundary, and electrode processes of polycrystalline ceramic material. The Kramers-Kronig data validation test was employed in the present impedance data analysis. Apart from the Nyquist (i.e., Z'' vs. Z') and Bode (i.e. $|Z|$ vs.) plots the alternative representations of impedance spectra were used to reveal contributions with relatively small differences in relaxation frequencies.

Keywords: mixed Aurivillius phase, ceramics, impedance spectroscopy

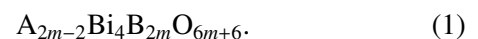
W niniejszej pracy zaprezentowano rezultaty badań poświęconych syntezie oraz wytworzeniu materiału ceramicznego należącego do grupy faz Aurivilliusa o mieszanej budowie i składzie chemicznym $\text{Bi}_5\text{TiNbWO}_{15}$. Materiał został zsyntezowany w wyniku reakcji w fazie stałej z mieszaniny proszków wyjściowych. Proces syntezy materiału ceramicznego badano z zastosowaniem różnicowej analizy termicznej (DTA) i analizy termogravimetrycznej (TG, DTG) oraz rentgenowskiej analizy strukturalnej. W wyniku badań rentgenowskich określono grupę przestrzenną $I2cm$ i parametry rombowej komórki elementarnej $a=5.4318\text{Å}$, $b=5.4255\text{Å}$, $c=41.6382\text{Å}$. Zastosowanie spektroskopii impedancyjnej pozwoliło na rozdzielenie wkładu ziaren, granic ziaren oraz procesów przyelektrodowych w impedancję polikrystalicznego materiału ceramicznego. W celu określenia spójności impedancyjnych danych pomiarowych przeprowadzono test Kramersa – Kroniga. Dane impedancyjne przedstawiono w postaci wykresów Nyquista (Z'' vs. Z'), wykresów Bode ($|Z|$ vs.) oraz alternatywnych sposobów prezentacji, które pozwoliły wyjawić wkład procesów polaryzacyjnych o zbliżonych częstotliwościach relaksacji.

1. Introduction

Due to growing interest in environmentally benign and energy-saving technologies, a new interest for the Aurivillius phases, which are generally formulated as $\text{A}_{m-1}\text{Bi}_2\text{B}_m\text{O}_{3m+3}$, has been generated [1]. The crystalline structure of the Aurivillius phases can be built according to the following general rule: first, the perovskite slabs containing (m) oxygen octahedrons [$\text{A}_{m-1}\text{B}_m\text{O}_{3m+1}$] along their thickness have to be cut out from a regular perovskite lattice by two planes of (001) type interleaved with fluorite-type bismuth-oxygen layers [Bi_2O_2]. Adjacent perovskite-like slabs are displaced in relation to each other for $a_0/\sqrt{2}$ in [100] direction, where a_0 – is a parameter of regular perovskite cell. In such an arrangement, the chains of m regular octahedrons along

the c -axis are interrupted by the $(\text{Bi}_2\text{O}_2)^{2-}$ layers, but form continuous chains along the plane perpendicular to the c -axis.

Sometimes perovskite layers which are sandwiched between $(\text{B}_2\text{O}_2)^{2+}$ layers have a different number of oxygen octahedrons: m' and m'' . When the difference between m' and m'' equals unity $|m' - m''| = 1$, the structure is a mixed bismuth layer type [2,3] and is generally described by the formula taking into account the average value of the parameter $m = (m' + m'')/2$ [4]:



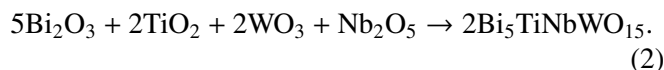
The aim of the present study was to fabricate $\text{Bi}_5\text{TiNbWO}_{15}$ (BTNW) ceramic material exhibiting the mixed Aurivillius structure [4, 5], investigate its crystalline structure and make use of impedance spec-

* UNIVERSITY OF SILESIA, DEPARTMENT OF MATERIALS SCIENCE, 41-200 SOSNOWIEC, 2 ŚNIEŻNA STR., POLAND

troscopy (IS) to gain a better insight into the all important conductivity phenomena in the bulk samples of BTNW. An alternative representation of IS spectra was used to analyze the data obtained [6].

2. Experimental

The mixed oxide method was employed for the ceramics fabrication. Commercially available TiO_2 , Bi_2O_3 , WO_3 , Nb_2O_5 powders were used as starting materials for preparation BTNW ceramics according to the solid phase reaction:



Sintering behavior of the powders was studied by simultaneous thermal analysis (STA). The measurements were obtained with the STA-409 Netzsch equipment – a combined DTA/TG/DTG system in which both thermal (DTA) and mass change effects (TG and DTG) are concurrently measured on the same sample. On the base of STA measurements (Fig.1) conditions of thermal processing of the stoichiometric mixture of starting oxide powders were chosen.

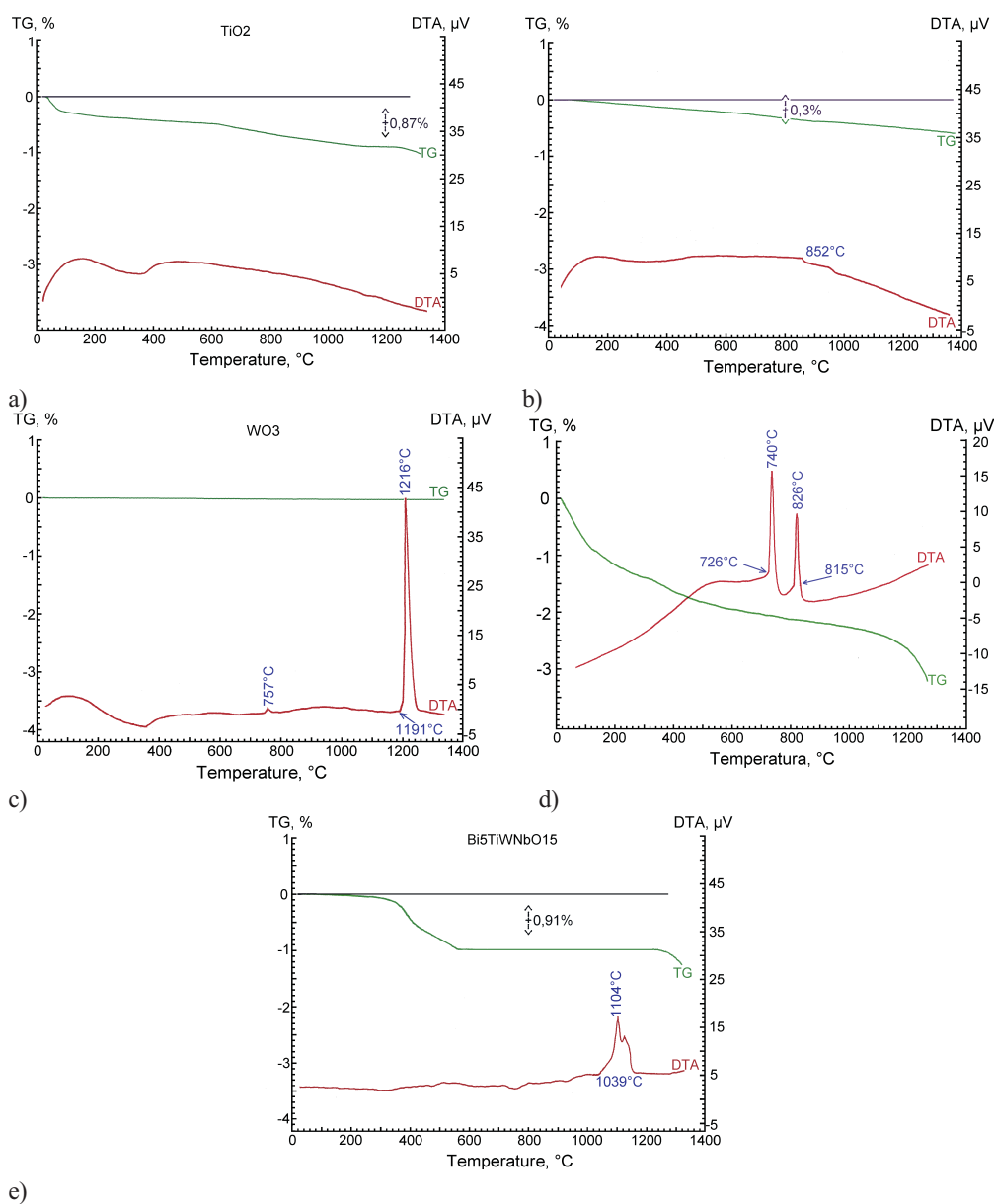


Fig. 1. Simultaneous thermal analysis for initial oxides, viz: TiO_2 (a), Nb_2O_5 (b), WO_3 (c) and Bi_2O_3 (d) as well as the stoichiometric mixture of these oxides used for preparation of bismuth-containing layered compound $\text{Bi}_5\text{TiNbWO}_{15}$ (e). Heating rate $10^\circ\text{C}/\text{min}$

After performing the STA analysis the powder was studied by X-ray diffraction (XRD). Crystalline structure of the ceramic powders was examined by XRD analysis, using the Philips PW 3710 X-ray diffractometer ($\Theta - 2\Theta$ method, $\text{CoK}_{\alpha 1\alpha 2}$ radiation, counting time 2s, step $\Delta 2\Theta = 0.02^\circ$) at room temperature. Analysis and fitting of the X-ray pattern was performed with the computer program PowderCell [7] equipped with the possibility of the Rietveld refinement.

BTNW ceramics was fabricated by ordinary sintering as well as sintering under pressure. Mixture of the starting powders was milled for 20 h and disk-shaped compacts of 1 cm in diameter were formed by pressing under pressure of $p=4\text{MPa}$. Calcination was carried out at $T_1 = 800^\circ\text{C}$ in a hermetic corundum crucible. After the calcination process the pellets were powdered, formed into disks and sintered twice at $T_2 = 1000^\circ\text{C}$ and $T_3 = 1030^\circ\text{C}$ for 3 hours each time.

In case of sintering under pressure (uniaxial hot pressing) the powder was calcined at $T = 800^\circ\text{C}$ and sintered at $T = 900^\circ\text{C}$ for $t=1$ h under pressure of $p=10\text{MPa}$. Mechanical treatment was applied to form 1 mm thick samples. To carry out the electrical measurements all samples were electroded by burning-in the silver paste at $T = 700^\circ\text{C}$.

Impedance measurements were carried out using a computer-controlled impedance analyser QuadTech-1920 in the frequency range from 20 Hz to 1 MHz. The impedance spectrum was recorded using an ac signal of amplitude 1 V at room temperature.

3. Results and discussion

One can see that in case of TiO_2 (Fig.1a) no thermal effects are present on DTA curve and mass loss is about 0.87% at $T = 1200^\circ\text{C}$. In case of Nb_2O_5 powder (Fig.1b) the mass loss was found 0.3% at $T=800^\circ\text{C}$ and a small exothermic peak may be seen at $T = 852^\circ\text{C}$. WO_3 powder showed no mass loss, however two exothermic peaks were detected namely, a small one at $T = 757^\circ\text{C}$ and strong one at $T = 1216^\circ\text{C}$ (Fig.1c). Bi_2O_3 powder showed two exothermic peaks at $T = 740^\circ\text{C}$ and $T = 826^\circ\text{C}$ with a total mass loss about 3% at $T = 1200^\circ\text{C}$ (Fig.1d). It is worth noting that four polymorphs of Bi_2O_3 have been reported in the literature, viz: α , β , γ , and δ -phases [8]. The phase transition from the monoclinic δ -phase, to the high temperature cubic -phase, at approximately $T = 730^\circ\text{C}$, has been observed. The δ -phase was also found to be stable up to its melting point of approximately $T=825^\circ\text{C}$ what is consistent with our measurements. In case of the stoichiometric mixture of powders the mass loss of about 0.91% takes place within the temperature range $T = 200 - 580^\circ\text{C}$ (Fig.1e)

which can be assigned to the chemical reaction proceed. The broad exothermic peak observed at $T = 1104^\circ\text{C}$ can be assigned to crystallization of a new phase of ceramic material. On the base of STA analysis a temperature of calcination $T = 800^\circ\text{C}$ was chosen which is higher than the end temperature of the mass change (Fig.1e).

It was found that in consequence of the temperature treatment within the range $T=20^\circ\text{C} - T = 1000^\circ\text{C}$ at the rate of $10^\circ\text{C}/\text{min}$ the volume fraction of $\text{Bi}_5\text{TiNbWO}_{15}$ phase amounts to 67%. (Fig.2). The remaining 33% by volume fraction was assigned to Bi_2WO_6 phase.

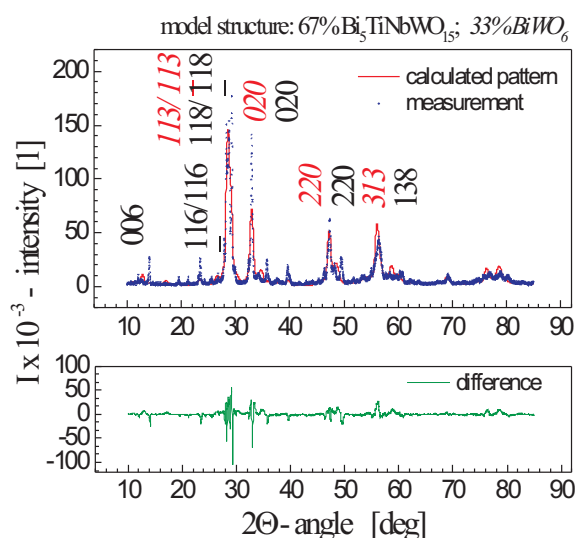


Fig. 2. X-ray diffraction pattern fitting for stoichiometric mixture of oxides after thermal analysis

Analysis of the X-ray diffraction pattern shows that suggested earlier elementary cells: orthorhombic [2] and tetragonal [4] do not describe completely observed diffraction lines. On the other hand, as far as $\text{Bi}_5\text{TiNbWO}_{15}$ exhibits ferroelectric properties at room temperature [4], from the two most suitable for characterization space groups, namely $Imcm$ (No.74) and $I2cm$ (No.46) [5,9], to describe the real crystalline structure of obtained $\text{Bi}_5\text{TiNbWO}_{15}$ ceramics the polar space group $I2cm$ was chosen (Fig.3). The calculations have shown that BTNW ceramics exhibits orthorhombic structure, space group $I2cm$ with the following parameters of the elementary cell: $a = 5.4318 \text{ \AA}$, $b = 5.4255 \text{ \AA}$, $c = 41.6382 \text{ \AA}$ (Fig.4). Parameters of the fitting procedure: $R_p=24.46\%$, $R_{wp}=39.22\%$, $R_{exp}=0.22\%$.

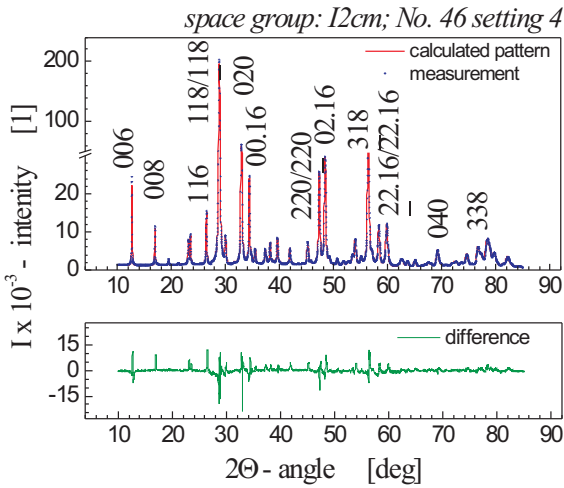


Fig. 3. X-ray diffraction pattern fitting for $\text{Bi}_5\text{TiNbWO}_{15}$ ceramics

The Arrhenius plot of conductivity for BTNW ceramics is shown in Fig.4. Apparently, the conductivity increases monotonously with temperature and changes by about six orders of magnitude in the regime of temperature studied. The activation energies have been calculated in the regions with differing slopes. In the low temperature regime it was found to be $E_a=0.34$ eV and in the high temperature region it was found to be $E_a=0.82$ eV. From the shape of the Arrhenius plot, the values of conductivity and the values of activation energies, it may be said that the conductivity is basically due to the oxygen vacancy motion [10].

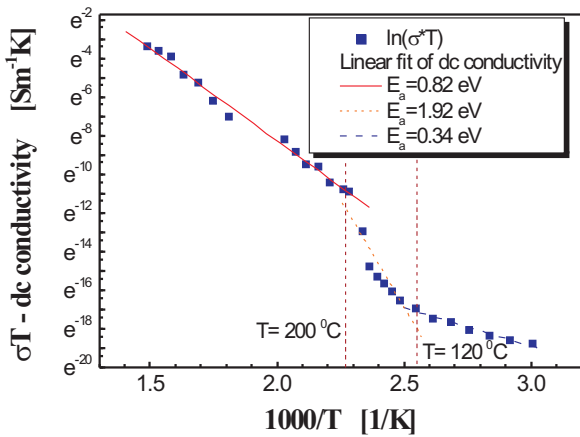


Fig. 4. Temperature dependence of the bulk electric conductivity for $\text{Bi}_5\text{TiNbWO}_{15}$ ceramics

A good understanding of bulk and grain boundary transport properties may be needed to assess the applicability of mixed Aurivillius phases for energy conversion systems, and to be able to optimize grain boundary controlled properties.

Thus, impedance spectroscopy was used to characterize the dynamic properties of BTNW ceramics. The contribution of various processes such as the electrode effects, bulk effects and the interfaces viz. the grain boundaries etc. [11] can all be resolved in the frequency domain.

Quality of impedance data is essential for proper analysis of dynamic properties of the material under investigation. The Kramers-Kronig (K-K) relations present a very useful tool for data validation [12]. They state that the imaginary part of a dispersion is completely determined by the form of the real part of the dispersion over the frequency range $0 \leq \nu \leq \infty$. Similarly the real part is determined by the imaginary dispersion form [13].

According to the method described in the literature [12, 13] and with the use of the computer program by B.Boukamp [12, 13] the K-K validation test was performed for BTNW impedance data. Results of residuals are given in Fig.5, whereas combination of the measured data and its K-K-transform are displayed in Fig.6. One can see that distribution of the residuals around the frequency axis has a random form (Fig.5). It indicates that the data is K-K compliant.

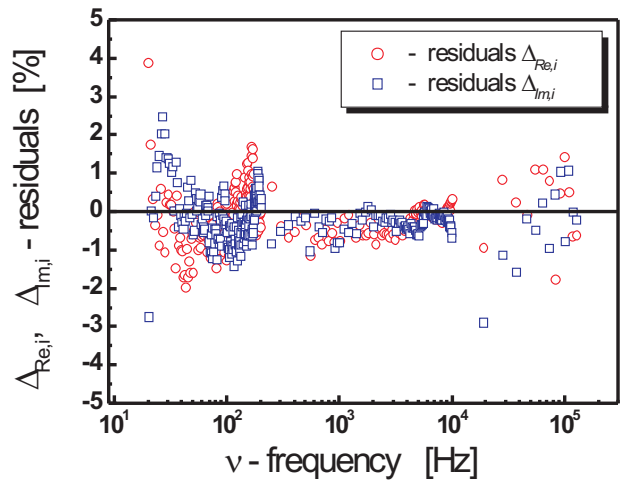


Fig. 5. Display of the Kramers-Kronig test residuals for the measured IS data

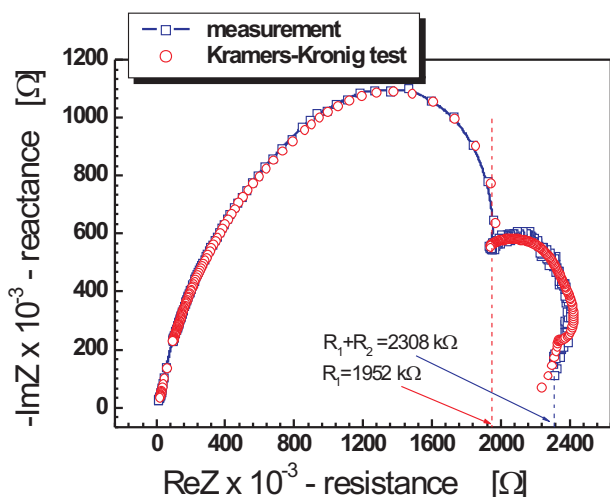


Fig. 6. Combination of the measured data and its Kramers-Kronig transform

The complex impedance plane plot of Z' versus Z'' (where Z' and Z'' are the real and imaginary parts of the complex impedance, respectively) given in Fig.7 is useful for determining the dominant resistance of the sample [14]. However, it is insensitive to smaller resistances. It shows the existence of two relaxation processes. Two overlapped impedance semicircles represent electrical phenomena due to bulk material and grain boundary effect [15].

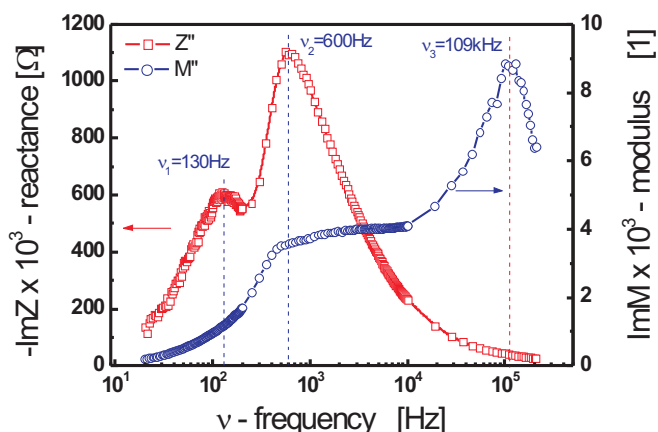


Fig. 7. Impedance Z'' and modulus M'' spectroscopic tests against frequency at room temperature

To determine relaxation frequencies the combined usage of impedance and modulus spectra were used (Fig.7). The power of combined usage of impedance and modulus spectroscopy is that the Z'' plot highlights phenomena with the largest resistance whereas M'' picks out those with smallest capacitances [10]. The relaxation frequencies determined from the combined spectra were as follows: the bulk relaxation frequency $\nu_B=109$ kHz, the grain boundary relaxation frequency $\nu_{gb}=600$ Hz and the electrode processes relaxation frequency $\nu_{el}=130$ Hz.

Other representations, especially Y'' vs. ν and $\tan\delta$ vs. ν , are considered in the present work and given in Fig.8. The $\tan\delta$ representation shows minima that can be attributed to grain boundary and electrode relaxation frequencies [16]. The peaks correspond to the bulk to grain boundary transition and grain boundary to electrode transition [16]. These frequencies are shown in Fig.8 by vertical lines. The representation of Y'' shows the electrode contribution with a peak at the expected electrode relaxation frequency, but is unable to reveal the high frequency (bulk) contribution.

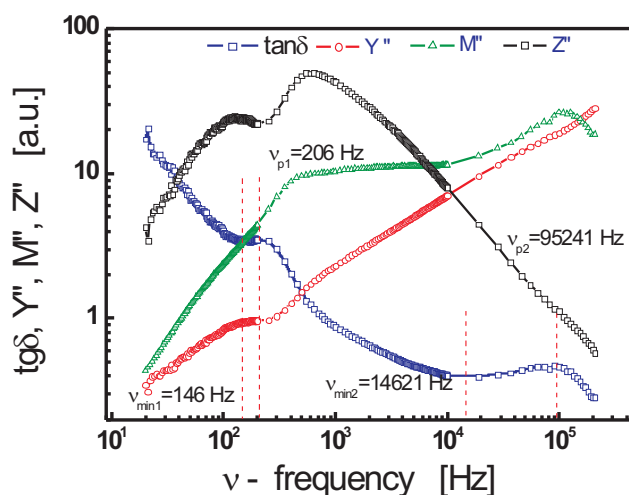


Fig. 8. Alternative representations of impedance Z'' , modulus, M'' , admittance Y'' and \tan for $\text{Bi}_5\text{TiWNbO}_{15}$ ceramics

4. Conclusions

As a result of the present studies $\text{Bi}_5\text{TiWNbWO}_{15}$ ceramics exhibiting the mixed Aurivillius structure have been obtained. The structure one can describe as orthorhombic, space group $I2cm$ with the following elementary cell parameters: $a = 5.4318\text{Å}$, $b = 5.4255\text{Å}$, $c = 41.6382\text{Å}$.

Impedance spectroscopy investigations have shown that dynamical properties of the polycrystalline ceramic system can be described by the equivalent electric circuit with three relaxation frequencies corresponding to bulk ($\nu_B=109$ kHz), grain boundary ($\nu_{gb}=600$ Hz) and electrode ($\nu_{el}=130$ Hz) contribution to the impedance spectra. Alternative representations of the spectroscopic data in a form of dispersion dependencies of \tan and imaginary part of admittance Y'' make it possible to determine transition regions between relaxation processes (i.e., electrode to grain boundary transition, and/or the grain boundary to bulk transition).

Acknowledgements

The present research has been supported by Polish Ministry of Education and Science from the funds for science in 2008-2011 as a research project N N507 446934.

REFERENCES

- [1] B. Aurivillius, *Ark. Khemi* **1**, 54, 463 (1949).
- [2] T. Kikuchi, A. Watanabe, K. Uchida, *Mat.Res. Bull.* **12**, 299 (1977).
- [3] T. Takenaka, K. Komura, K. Sakata, *Jap.J.Appl.Phys.* **35**, 5080 (1996).
- [4] A. Lisińska-Czekaj, D. Czekaj, Z. Surowiak, J. Ilczuk, J. Plewa, A. V. Leyderman, E. S. Gagarina, A. T. Shuvaev, E. G. Fesenko, *J.Eur.Ceram.Soc.* **24**, 947 (2004).
- [5] A. Snedden, D. O. Charkin, V. A. Dolgikh, P. Lightfoot, *J.Solid State Chem.* **178**, 180 (2005).
- [6] J. C. C. Abrantes, J. A. Labrincha, J. R. Frade, *Mater. Res. Bull.* **35**, 727 (2000).
- [7] W. Kraus, G. Nolze, *J. Appl. Cryst.* **29**, 301 (1996).
- [8] N. M. Sammes, G. A. Tompsett, H. Nafe, F. Aldinger, *J.Europ. Ceram. Soc.* **19**, 1801 (1999).
- [9] P. Boullay, G. Trolliard, D. Mercurio, J. M. Perez-Mato, L. Elcoro, *J.Solid State Chem.* **164**, 252 (2002).
- [10] A. R. James, S. Balaji, S. B. Krupanidhi, *Mat. Sci. Eng.* **B64**, 149 (1999).
- [11] J. E. Bauerle, *J Phys. Chem. Solids* **30**, 2657 (1969).
- [12] B. A. Boukamp, *J. Electrochem. Soc.* **142**, 1885 (1995).
- [13] B. A. Boukamp, *Solid State Ionics* **169**, 65 (2004).
- [14] D. Czekaj, A. Lisińska-Czekaj, T. Orkisz, J. Orkisz, G. Smalarz, *J. Eur. Ceram. Soc.* (2009), doi: 10.1016/j.jeurceramsoc.2009.06.036.
- [15] Z. G. Yi, Y. X. Li, Y. Wang, Q. R. Yin, *Appl.Phys.Lett.* **88**, 162908 (2006).
- [16] J. C. C. Abrantes, J. A. Labrincha, J. R. Frade, *Mater. Res. Bull.* **35**, 965 (2000).

Received: 10 October 2009.